Immunoreactivity for calcium-binding proteins defines subregions of the vestibular nuclear complex of the cat

Joan S. Baizer and **James F. Baker**

Department of Physiology and Biophysics, School of Medicine and Biomedical Sciences, University at Buffalo, 123 Sherman Hall, Buffalo, NY 14214-3078, USA.

Department of Physiology and Institute for Neuroscience, Physiology/Medical, Ward 5-071, M211, Northwestern University Medical School, 303 East Chicago Avenue, Chicago, IL 60611-3008, USA

Abstract

The vestibular nuclear complex (VNC) is classically divided into four nuclei on the basis of cytoarchitectonics. However, anatomical data on the distribution of afferents to the VNC and the distribution of cells of origin of different efferent pathways suggest a more complex internal organization. Immunoreactivity for calcium-binding proteins has proven useful in many areas of the brain for revealing structure not visible with cell, fiber or Golgi stains. We have looked at the VNC of the cat using immunoreactivity for the calcium-binding proteins calbindin, calretinin and parvalbumin. Immunoreactivity for calretinin revealed a small, intensely stained region of cell bodies and processes just beneath the fourth ventricle in the medial vestibular nucleus. A presumably homologous region has been described in rodents. The calretinin-immunoreactive cells in this region were also immunoreactive for choline acetyltransferase. Evidence from other studies suggests that the calretinin region contributes to pathways involved in eye movement modulation but not generation. There were focal dense regions of fibers immunoreactive to calbindin in the medial and inferior nuclei, with an especially dense region of label at the border of the medial nucleus and the nucleus prepositus hypoglossi. There is anatomical evidence that suggests that the likely source of these calbindin-immunoreactive fibers is the flocculus of the cerebellum. The distribution of calbindin-immunoreactive fibers in the lateral and superior nuclei was much more uniform. Immunoreactivity to parvalbumin was widespread in fibers distributed throughout the VNC. The results suggest that neurochemical techniques may help to reveal the internal complexity in VNC organization.

Keywords

Vestibular nerve; Calbindin; Calretinin; Parvalbumin; Purkinje cells; Flocculus; Nodulus

Abbreviations

BC: brachium conjunctivum; BP: brachium pontis; CD: dorsal cochlear nucleus; CGL: cochlear granular layer; CUR: cuneate nucleus, rostral division; CVA: ventral cochlear nucleus; CX: external cuneate nucleus; DMV: dorsal motor nucleus of the vagus; FTG: gigantocellular tegmental field of the reticular formation; FTL: lateral tegmental field of the reticular formation; INT: nucleus intercalatus; MLF: medial longitudinal fasciculus; PT: pyramidal tract; PH: nucleus prepositus hypoglossi; RB: restiform body; S: solitary tract; SA: stria acoustica; SM: medial nucleus of the solitary tract; TB: trapezoid body; VIN: inferior vestibular nucleus; VLD: lateral vestibular nucleus, dorsal division; VLV: lateral vestibular nucleus, ventral division; VMN: medial vestibular nucleus;

E-mail: baizer@buffalo.edu.

VNC: vestibular nuclear complex; VSL: superior vestibular nucleus, lateral division; VSM: superior vestibular nucleus, medial division; 5P: principal sensory trigeminal nucleus; 5SM: alaminar spinal trigeminal nucleus, magnocellular division; 5ST: spinal trigeminal tract; 6: sixth cranial nerve nucleus; 7N: seventh cranial nerve; 7G: genu of the seventh cranial nerve; 8N: eighth cranial nerve; 12: twelfth cranial nerve nucleus

Introduction

The vestibular nuclear complex (VNC) is classically divided into four major nuclei and several smaller cell groups on the basis of cytoarchitectonics (Brodal and Pompeiano 1957; Berman 1968; Brodal 1984). There is evidence supporting the idea that these nuclei are functionally distinct. Studies of the superior vestibular nucleus have explored its role in mediating the vestibuloocular reflex (Highstein and Ito 1971; Mitsacos et al. 1983; Zhang et al. 1993, 1995). By contrast, studies on the lateral vestibular nucleus have focused on its influences on neck and limb muscles (Shamboul 1980; Akaike 1983; Boyle et al. 1996; Kuze et al. 1999; Boyle 2000; Leblond et al. 2000; Krutki et al. 2003).

However, both anatomical and physiological data suggest a more complex organization of the VNC than a simple division into four nuclei, each with a different function. There is evidence both for functional subdivisions within each nucleus, and for overlapping functions among the nuclei. First, no major input is restricted only to a single nucleus. For example, the vestibular nerve projects to all four nuclei of the VNC (Korte 1979; Carleton and Carpenter 1984; Siegborn et al. 1991; Newlands and Perachio 2003), and each of the nuclei receives afferent fibers from each of the semicircular canals and otoliths (Sato and Sasaki 1993; Imagawa et al. 1995; Naito et al. 1995; Newlands and Perachio 2003). In fact, single vestibular neurons may receive convergent input from more than one sensory structure (Baker et al. 1984; Zhang et al. 2001; Dickman and Angelaki 2002; Newlands and Perachio 2003). Second, no major output arises from cells confined to only one of the nuclei. For example, vestibulospinal fibers arise from cells in the inferior and medial vestibular nuclei as well as from the lateral nucleus (Peterson and Coulter 1977; Akaike 1983; Bankoul and Neuhuber 1992; Donevan et al. 1992; Rose et al. 1996; McCrea et al. 1999; Wilson and Schor 1999). Third, within each nucleus, afferent fibers from different sensory structures are not uniformly distributed but found in restricted regions (Imagawa et al. 1995; Naito et al. 1995). Fourth, cells of origin of efferent pathways are not uniformly distributed within a nucleus. For example, the vestibulospinal neurons in the inferior and medial nuclei are found only in restricted regions (Rose et al. 1996; Wilson and Schor 1999). The same principles apply to all of the other connections of the VNC (reviews in Wilson and Melvill Jones 1979; Gerrits 1990; Barmack 2003). Finally, cells with similar response properties may be found in more than one vestibular nucleus (examples in McCrea et al. 1987a, 1987b).

The complexity of VNC organization has long been recognized (Brodal and Pompeiano 1957; Taber 1961; Berman 1968; Hauglie-Hanssen 1968), as was the fact that the appearance of the VNC in cell, Golgi, or fiber stains does not reflect this complexity. In other regions of the central nervous system, neurochemical techniques, including enzyme histochemistry and immunohistochemistry, have shown anatomical subdivisions not apparent in cell or fiber stains. Examples include staining for cytochrome oxidase in visual cortex (Horton and Hubel 1981), and acetylcholinesterase in the superior colliculus and striatum (Graybiel and Ragsdale 1978; Graybiel 1983; Chevalier and Mana 2000), immunoreactivity to nitric oxide synthase in the nucleus prepositus hypoglossi (Moreno-Lopez et al. 2001), immunoreactivity to zebrin in the cerebellum (Sillitoe et al. 2003), and immunoreactivity to calcium-binding proteins in thalamus and cortex (Rausell and Jones 1991a, 1991b; Rausell et al. 1992; Cusick et al. 1993; de Venecia et al. 1995; Jones et al. 1995).

Data from rodents suggest that this approach may be useful for the VNC as well. Studies using immunoreactivity to calcium-binding proteins noted a small region of calretinin-immunoreactive cells in the medial vestibular nucleus, and further found that immunoreactivity to parvalbumin and calbindin defined different fiber populations (Arai et al. 1991; Résibois and Rogers 1992; Kevetter and Leonard 1997; Paxinos et al. 1999). We have extended this approach to the cat, an animal widely used in studies of vestibular anatomy, physiology and behavior (references in Wilson and Melvill Jones 1979; Gerrits 1990; Wilson et al. 1999; Barmack 2003). We found a calretinin-immunoreactive cell group in the medial nucleus, and also evidence that the cells are cholinergic. We also found limited regions of dense immunoreactivity for calbindin in fibers in the medial and inferior nuclei. We have presented brief reports of some of these results (Baizer and Baker 2000, 2001).

Materials and methods

All experiments followed the principles of laboratory animal care set forth by the National Institutes of Health in the Guide for Care and Use of Laboratory Animals and were approved by the Institutional Animal Care and Use Committee at Northwestern University.

Tissue preparation

Six cats were deeply anesthetized with Nembutal and then perfused through the aorta with saline followed by 4% paraformaldehyde in phosphate-buffered saline (PBS). The brains were removed, and the brainstem dissected from the rest of the brain. In all but one case the cerebellum was also dissected free. The brainstems were then cryoprotected in graded concentrations of sucrose in PBS (10%, 20%, and 30%), quick frozen in −70 °C isopentane or a frozen solution of 30% ethylene glycol and 30% glycerol in PBS, and the frozen blocks covered with that solution and stored in a −70 °C freezer until cutting. The brainstem of one case was first embedded in an albumin-gelatin matrix. 50 μm frozen frontal (five cases) or 40 μm horizontal (one case) sections of the brainstems were cut on a sliding microtome. Sections were stored at −20 °C in tissue culture wells in 30% ethylene glycol and 30% glycerol in PBS.

Immunohistochemistry

Sections from 3–5 cases were incubated with each antibody and immunoreactivity visualized using standard immunohistochemical techniques (Hockfield 1993). Briefly, sections were removed from the cryoprotectant, rinsed in PBS and incubated in a solution of PBS or PBS with 5% nonfat dry milk, 0.3% Triton-X100, 1–1.5% normal serum (Vector Laboratories, Burlingame, CA), and the primary antibody overnight on a tissue shaker at 4°. For calretinin we initially used a monoclonal antibody (Chemicon, MAB1568, 1:2500); data using this antibody are shown in Figs. 1, 3, 5, 7, and 8. We confirmed the basic observations with a polyclonal antibody (Chemicon, AB149, 1:2500); data using this antibody are shown in Fig. 2. For calbindin, we initially used a monoclonal antibody (Sigma, c8666, 1:2500); data are shown in Fig. 4. We then confirmed the basic staining pattern with a polyclonal (Chemicon, AB1778, 1:2000; preabsorbed against calretinin) antibody; data using the polyclonal antibody are shown in Figs. 5, 7, and 8. Additional antibodies used were a monoclonal to parvalbumin (Sigma, P-3171, 1:2500) and a polyclonal antibody to choline acetyltransferase (ChAT, Chemicon, AB 143,1:1000). Sections were then processed using a Vector ABC Elite kit with the appropriate secondary antibody (mouse, rabbit, or Universal kits) and then the ABC solution. Immunoreactivity was visualized by incubating sections in 3,3′-diaminobenzidine (DAB, Sigma) with 0.0015–0.003% H_2O_2 in dilute PBS. Staining on some sections was enhanced with the addition of nickel ammonium sulfate and cobalt chloride or nickel ammonium sulfate alone to the DAB solution (Adams 1981). For a few sections, we used Vector VIP or NovaRed as a substrate instead of DAB. Four control sections from each case were processed with the primary antibody omitted from the initial solution and then with a

mouse or a rabbit secondary antibody. No immunostaining was seen when the primary antibody was omitted. Two additional control sections from each case were incubated in DAB alone to assess the presence of endogenous peroxidase activity. There was virtually no endogenous peroxidase activity, and we therefore did not include a quenching procedure.

To examine the possible colocalization of calretinin and ChAT, we simultaneously incubated six sections from the case with the attached cerebellum with the mouse monoclonal antibody to calretinin and the rabbit polyclonal antibody to ChAT, and then with Alexa fluorescent secondary antibodies (Molecular Probes, Eugene, Oregon), a goat anti-mouse Alexa 488 to label calretinin, and a goat anti-rabbit Alexa 594 to label ChAT. To show the relative distributions of calretinin and calbindin immunoreactivity, two sections were incubated simultaneously with the mouse monoclonal antibody to calretinin and the rabbit antibody to calbindin, and then labeled with the fluorescent secondary antibodies as above.

Data analysis and photography

We used the Berman (1968) atlas of the cat brainstem to determine the approximate stereotaxic anterior-posterior (A-P) or dorso-ventral (D-V) levels of coronal and horizontal sections. We also follow his terminology and abbreviations for the four nuclei of the VNC, the medial (VMN), inferior (VIN), the lateral (dorsal subdivision VLD, ventral subdivision, VLV) and the superior (medial subdivision VSM, lateral subdivision VSL) nuclei, and other brainstem structures. For each case, a set of sections 1 mm apart was stained with cresyl violet to aid in locating structures.

Frontal sections from P13 to P4 were examined under a light microscope. The locations of labeled cells in the VNC, the neighboring nucleus prepositus hypoglossi (PH), the medial longitudinal fasciculus (MLF), and the reticular formation were plotted onto outline drawings of sections about 1 mm apart using MDPlot software (Accustage, Shoreview, MN). Digital images of selected sections were captured using a Spot RT CCD video camera (1520×1080 pixels, Diagnostic Instruments, Sterling Heights, MI) mounted on a Nikon Eclipse 800 microscope. Fluorescent sections were photographed through a BioradMRC-1024 confocal imaging systemoperating on a Nikon Optiphot microscope, or with the fluorescent optics of the Nikon Eclipse 800 microscope. Each confocal image consisted of a *z*-stack of pictures taken at a depth interval of 1 μm and then projected into one image using Confocal Assistant software. For the figures, images were adjusted for brightness and contrast using Adobe Photoshop, and plates assembled using that software. Section outlines were drawn with CorelDraw software.

Results

The labeling pattern in the VNC for each of the three calcium-binding proteins is distinctly different, and we will describe results for each separately. In addition to analyzing the labeling in the VNC proper, we also looked at label in the neighboring and functionally-related nucleus PH (Baker and Berthoz 1975; Kaneko 1997, 1999), the reticular formation, the MLF, and the eighth nerve as it enters the brainstem, and we will describe the labeling pattern for those regions as well.

Calretinin

With both the monoclonal and the polyclonal antibodies to calretinin there is very little labeling in the brainstem overall, with only scattered fibers and a few cells labeled in the VNC. However, there is an intensely labeled region of calretinin-immunoreactive cells, puncta, and processes just under the ventricle, centered at 2.5–3.0 mm lateral to the midline; we shall refer to this region as the calretinin-immunoreactive area or, more simply, the calretinin area. Figure 1A illustrates the location, size and extent of the calretinin area on seven drawings of sections from

about P12 to P5; these drawings are based on its appearance in sections incubated with the monoclonal antibody, three of which are illustrated in Fig. 1B–E. The calretinin area is first seen at the posterior limit of the VMN, at a stereotaxic level of about P11, and continues to the anterior limit of that nucleus, at about P6. At its posterior limit it is located relatively laterally in the VMN; from about P9 it extends medially to the border with PH. The calretinin area varies in size over its anterior-posterior extent. It is the largest at about P8–9, where it extends about 1–2 mm in the medio-lateral (M-L) direction, and 1–2 mm in the dorso-ventral direction, and smaller at more anterior and posterior levels. At its largest, the area consists of a more darkly stained central region adjoining the ventricle, surrounded laterally, medially, and ventrally by a more lightly stained region. Both regions are included in the shaded areas in A. Figures 1C and D illustrate the size and shape of cells and processes in the calretinin area. Labeled cells in the central region are relatively small, with 10–15 μm-diameter round or oval cell bodies. Most processes cannot be followed far from the cell body in this plane of section. Neurons in the surrounding region are larger, with pyramidal or polygonal cell bodies. The staining of the processes of these cells is more extensive (compare cells and processes in the upper left and lower right in Fig. 1D).

In addition to the region of dense calretinin label in the medial nucleus, there are a few labeled cells elsewhere in the medial nucleus and in the inferior nucleus (Fig. 1B,C). At levels of P7–P6 a few labeled cells are seen in the region where vestibular efferent neurons are found (Gacek and Lyon 1974). At this level, a few calretinin-immunoreactive cells are seen in the superior and lateral nuclei. Calretinin also labels a few neurons in PH (Fig. 1B,C,E). There are large calretinin-immunoreactive cells in the gigantocellular terminal field of the reticular formation (FTG, Fig. 1E). Small-diameter fibers run between the calretinin-immunoreactive region and the reticular formation. Some cells in the abducens nucleus are calretinin-immunoreactive (Fig. 1E), and an occasional labeled cell is seen embedded in the fibers of the MLF.

Figure 2A shows the calretinin area (between the arrows) on a horizontal section at about the level of −3.4. In this section the calretinin area extends about 4 mm in the A-P direction, and the change in width at different A-P levels is clear. The larger magnification photomicrograph in Fig. 2B shows cells and processes in the calretinin area, and illustrates a pronounced tendency for processes to extend in the A-P direction. Several fusiform cells are visible (arrowhead), with cell bodies also aligned in an A-P orientation. Such cells would appear to have round or oval cell bodies and short processes in sections cut in the frontal plane, as was observed. An immunoreactive cell in PH (Fig. 2B, arrow) is also visible.

Calretinin-immunoreactivity thus distinguishes a clear subregion of the medial vestibular nucleus. Barmack described many ChAT-immunoreactive cells dorsally in the VNC of the rabbit (Barmack et al. 1992b, 1992c). The location of these cells appears to overlap the calretinin area, raising the possibility that some of the calretinin-immunoreactive cells might be cholinergic. We find, as in rabbit, that many cells in the dorsal VNC are ChAT-immunoreactive. The region over which ChAT-immunoreactive cells are found is larger than, but includes, the calretinin area. In sections double-labeled for calretinin and ChAT, all cells that are clearly calretinin-immunoreactive are also immunoreactive for ChAT (Fig. 3). ChAT-immunoreactivity labels only cell bodies (Fig. 3A), whereas calretinin-immunoreactivity labels both cell bodies and processes (Fig. 3B). Each calretinin-immunoreactive cell body can also be identified as ChAT-immunoreactive (see arrows in Fig. 3A,B). There are many ChAT-immunoreactive cell bodies both within and outside of the calretinin region that are not calretinin-immunoreactive (arrowheads in Fig. 3A).

Calbindin

With both the monoclonal or the polyclonal antibody to calbindin there is heavy labeling of fibers and terminals, with fibers, cross-sections of fibers, and puncta seen throughout the VNC

(Fig. 4A–C). In the three animals examined, there are regions of denser label in VIN and VMN, the size and location of which change over their anterior-posterior extent. Most posteriorly at about P12, there is a small region of dense label just along the ventricle in VIN. Slightly more anteriorly, at about P11.5, a second small region of dense label is seen at the medial edge of the VMN at the border of PH. At about P11, the medial region appears as a dark patch roughly trapezoidal in shape (Fig. 4A, arrow). The lateral patch is still visible beneath the ventricle, and there is also patchy label in the VIN. At about P9–P10 there is a single dorso-ventrally-oriented streak of darker label. At P9–P8 there are two spots of label medially in VMN, as well as a dark patch along the ventricle (Fig. 4B). At the level of the genu of the seventh nerve (P7) there is a patchy distribution of labeled fibers in the lateral vestibular nucleus and uniform label in the medial nucleus. At the level of the seventh nerve (P6), dense, patchy label is seen in the superior vestibular nucleus (Fig. 4C). In order to determine the three-dimensional organization of the darker patches of label one would have to trace them on very closely spaced sections, a task we have not yet undertaken. There are also scattered labeled cells in each of the nuclei, including a population of large cells in the dorsal division of the lateral nucleus.

Calbindin labels a few cells as well as a few fibers in PH (Fig. 4A–C). In the reticular formation, the pattern of label also changes dramatically at different A-P levels. At about P11 there is a dense, circumscribed region of reticular cell and fiber label just ventral to the VMN (Figs. 4A and 5, arrowheads), in a region relatively free of calretinin label (Fig. 5). At about P10 there is a small cluster of labeled cells just ventral to PH. More anteriorly, at about P9.5–8.5, there is a small cluster of large labeled cells among the fibers of the MLF dorsally (Fig. 4B, arrow).

Calretinin and calbindin thus both deffne areas of dense label. In order to see the relation of the calretinin area and the regions of dense calbindin fiber label, we looked at sections double-labeled for the two proteins (Sigma, MAB1568 calretinin; Chemicon, AB1778, calbindin). Figure 5 shows that the dense calbindin-immunoreactive triangular patch (red) is medial to the calretinin-immunoreactive area (green) at about P11. However, there are calbindin-immunoreactive fibers overlapping the calretinin area, and a scattering of calbindin-immunoreactive fibers in PH. The overall appearance of each label in the fluorescent material was very similar to that seen on the single-labeled sections in which immunoreactivity was visualized with DAB.

Parvalbumin

Parvalbumin-immunoreactivity is extensive in fibers and puncta throughout the VNC. The fiber labeling is more uniform than with calbindin, and about equally dense in all four nuclei and PH. Beginning at the most posterior extent of the VNC at about P12 and continuing to P9–10 there is heavy fiber label in VMN and VIN, with a few labeled cells in each nucleus (Fig. 6A). The fiber labeling is most dense just along the ventricle. There is slightly darker parvalbumin label at the border of VMN and PH in the region of the heavy calbindin labeling (Fig. 6A, arrow). The bundles of fibers running through the VIN in an A-P direction, seen as cross-sections, are stained. More anteriorly, at the level of the genu of the seventh nerve, there are labeled fibers throughout the lateral nucleus (Fig. 6C), and there are many labeled fibers cut in cross-section. More anteriorly still, there are dense labeled fibers in the superior nucleus (Fig. 6D). The density of fiber label in PH is about the same as in the VNC (Fig. 6A–D).

Label of fibers posteriorly in the reticular formation with parvalbumin is very sparse (Fig. 6A,B). There are scattered labeled cells in the reticular formation, in both the FTG and the lateral tegmental field (FTL), and there are also some cells embedded in the MLF.

MLF, commissural fibers, eighth nerve

We also examined the pattern of staining in the fibers of the MLF. In coronal sections, the MLF contains many fibers cut in cross-section, as well as some longer segments. The pattern of labeling differs among the three proteins. Calretinin labeled cross-sections of fibers in the dorsal MLF over the entire anterior-posterior extent of the VNC (Fig. 1B–D; Fig. 7A,C). Calretinin-immunoreactive fibers in the MLF are seen at levels anterior to the VNC. In addition, a few calretinin-immunoreactive fine fibers appear to extend medially from the calretinin area, weave across the MLF, and traverse the midline (Fig. 7A,C). These fibers are seen over an A-P range of about P10–P7. Calbindin-immunoreactivity shows short labeled fibers oriented in a dorsal-ventral direction. There are also a few small caliber calbindin-immunoreactive fibers crossing the MLF (Fig. 7D; polyclonal antibody). Parvalbumin immunoreactivity also labels many cross-sections of fibers over the entire dorsal-ventral extent of the MLF, at all A-P levels (Fig. 7B, arrowheads). Very few such fibers are seen with calbindin.

In frontal sections at about P7, fibers of the eighth nerve are seen sweeping dorsomedially through the brainstem (Fig. 8D). Thick labeled fibers are seen in the eighth nerve with all three of the calcium-binding proteins; there are no major differences in density among them (Fig. 8A–C). For each protein, labeled fibers are scattered about in the nerve rather than grouped together.

Discussion

We find focal regions of heavier label within the VMN and VIN with two of the three calcium-binding proteins. Calretinin immunoreactivity defines a cellular region, while calbindin immunoreactivity is predominantly in fibers. Label with parvalbumin is again largely in fibers and much more uniform across the VNC. Immunoreactivity to calcium-binding proteins in the VNC has been analyzed in several reports in the rodent, and we will review similarities and differences between those findings and our results in the cat. We will also consider the likely sources of the calbindin and parvalbumin immunoreactive fibers seen in the VNC. The functions of the regions defined by calretinin and calbindin immunoreactivity are a matter of speculation at present. We will discuss data on inputs to and projections from those regions that may help illuminate their role in vestibular reflexes.

Calcium-binding proteins in rodent brainstem

Two studies (Arai et al. 1991; Résibois and Rogers 1992) have looked at calretinin-immunoreactivity in the vestibular nuclear complex of rodent, one study at calbindin and parvalbumin (Celio 1990) and two studies at all three proteins (Kevetter 1996; Paxinos et al. 1999). There are minor differences among results in different studies in rodent, presumably reflecting differences in antibodies or methods. In general, the results for calretinin and parvalbumin are similar in cat and rodent, while the pattern for calbindin is less so.

Calretinin—We find few calretinin-immunoreactive fibers in the brainstem overall including the VNC, in agreement with the sections shown by Paxinos et al. (1999). A region of dense calretinin cell and fiber immunoreactivity under the ventricle in the medial vestibular nucleus was seen in all rodent studies. We also see a few calretinin-immunoreactive cells scattered across the VNC and reticular formation. Other reports are inconsistent in descriptions of labeled cells, with cells reported in all nuclei in two studies (Arai et al. 1991; Paxinos et al. 1999), all but the lateral nucleus in another (Résibois and Rogers 1992), and all but the superior vestibular nucleus in a fourth (Kevetter 1996). We see labeled fibers in the MLF and eighth nerve and labeled cells in the reticular formation, in agreement with all studies in the rodent. Kevetter (1996) noted that stained fibers could be traced from the calretinin area across the midline, in

agreement with our observation of calretinin-immunoreactive fibers crossing the midline in the cat.

Calbindin—We see widespread fiber labeling in the VNC, with restricted denser patches at more posterior levels in the medial and inferior nuclei, and more uniform label more anteriorly in the lateral and superior nuclei. Widespread calbindin fiber label has also been seen in all rodent studies, with some disagreement about the presence and locus of darker patches. Kevetter (1996) emphasized the similarity of calbindin and parvalbumin staining but did mention more dense calbindin fiber and terminal label in VMN under the ventricle and also at the medial border of VMN and PH. However, the atlas of Paxinos et al. distinguishes two subdivisions of the medial vestibular nucleus with calbindin staining. These divisions do not appear similar to the pattern in cat, and the dense patch at the border of VMN and PH that we see in cat is not apparent in their illustrations. We also saw scattered labeled cells in the VNC. Again different reports vary, from reports of calbindin-labeled cells in all nuclei (Paxinos et al. 1999), cells only in VMN and VIN (Saxon and Beitz 2000) and few or no calbindin-labeled cells (Celio 1990; Kevetter 1996). The differences between our findings in the cat and other studies in the rodent are thus no greater than variability among rodent studies, suggesting that there may not be major species differences in calbindin labeling of cells. A few calbindin-labeled cells in the reticular formation and in PH were shown by Paxinos et al. (1999). All studies agree that a population of eighth nerve fibers is labeled with calbindin.

Parvalbumin—The widespread and uniform pattern of parvalbumin-immunoreactive fiber label in the eighth nerve and VNC in the cat is similar to that in all studies in rodent. We see scattered parvalbumin-immunoreactive cells in the VNC, as did one rodent study (Paxinos et al. 1999). Label in PH similar to that in the VNC is shown by Kevetter (1996, Fig. 3C), however in the pictures of Paxinos et al. (1999) the label in PH is much lighter than in the VNC (Fig. 155). Labeled fibers in the MLF are illustrated in the Paxinos atlas and in the study of Celio (1990). Labeled cells in the reticular formation and MLF are shown by Paxinos et al. (1999), whereas Kevetter (1996) found no labeled cells in the MLF.

The fiber label in the eighth nerve in cat appears about equal with each of the three antibodies. While all studies in rodents report fibers immunoreactive for each protein, there are major differences in the relative numbers of fibers immunoreactive for the different proteins, and the degree of colocalization. The significance of these differences cannot be evaluated in the absence of standardized methods and more quantitative data analysis.

ChAT—We see a population of ChAT-immunoreactive cells in the dorsal VNC, and present evidence that cells of the calretinin-area colocalize ChAT and calretinin. ChAT-immunoreactive cells in the VNC have been described in rabbit and rodent (Barmack et al. 1992b, 1992c), and in one study (Carpenter et al. 1990), but not another (Kimura et al. 1981) in the cat. No previous studies analyzed the possible colocalization of ChAT and any of the calcium-binding proteins.

Sources of calretinin, calbindin, and parvalbumin fibers

For all three calcium-binding proteins, the eighth nerve is one source of immunoreactive fibers in the VNC. For calbindin and parvalbumin, but not calretinin, a second major source is Purkinje cells of the cerebellum (Celio 1990). Work in the rodent suggests that the cerebellum and the eighth nerve are in fact the only sources of calbindin-immunoreactive fibers in the VNC (Kevetter and Leonard 1997; Bäurle et al. 1998). The possible sources of parvalbumin-immunoreactive fibers are more numerous, as several brainstem structures with parvalbumin-immunoreactive cells, including the interstitial nucleus of Cajal (Kokkoroyannis et al. 1996; Horn et al. 1999), the rostral interstitial nucleus of the MLF (Horn and Büttner-Ennever

1998) and inhibitory and excitatory burst neurons of the reticular formation (Horn et al. 1995) may contribute the parvalbumin-immunoreactive fibers that are seen in the MLF and VNC.

Functional considerations

Calcium-binding proteins—Calcium-binding proteins have been proven to be useful markers of specific cell and fiber populations in diverse locations within the nervous system. For example, calretinin-immunoreactive neurons have been found in the retina (Jeon and Jeon 1998), the hippocampus (Murakawa and Kosaka 1999), the cerebellum (Fortin et al. 1998), and are a sub-population of GABAergic neurons in cerebral cortex (Condéet al. 1994). The calcium-binding protein associated with a given neurotransmitter varies. Purkinje cells, which are GABAergic, do not contain calretinin (Arai et al. 1991; Résibois and Rogers 1992; Rogers and Résibois 1992; Edmonds et al. 2000), and do colocalize parvalbumin and calbindin (Batini 1990; Celio 1990). In cerebral cortex each calcium-binding protein is found in a separate population of GABAergic interneurons (Van Brederode et al. 1990), and in the vestibular nerve, the three proteins are present in three different populations of glutamatergic fibers (Carpenter et al. 1990). Physiological roles of the different calcium-binding proteins are still debated (Arai et al. 1991; Baimbridge et al. 1992; Rogers and Résibois 1992). Their calcium buffering capacity could influence diverse functions, segregating signaling pathways by limiting calcium diffusion (Roberts 1993, 1994; Lenzi and Roberts 1994). It is possible the regulation of response timing by calcium-binding proteins that occurs in frog saccular hair cells (Edmonds et al. 2000) is also relevant to the much longer time course of central vestibular mechanisms.

Calretinin area—At present, we do not know either the response properties or connections of the cells in the calretinin area. Inferences about the function of the area can be made only on the basis of anatomical studies that examined connections of the general territory of the calretinin area. While there are some data in cat, there are also pertinent studies in other species. In interpreting these data it is also necessary to remember that the calretinin-immunoreactive cells are interspersed with other cells that may not have the same pattern of connections. However, the evidence is strong enough to suggest some general ideas about the possible functions of the calretinin area. First, it is clear that the calretinin area of the VMN receives direct vestibular nerve input (Korte 1979; Carleton and Carpenter 1984; Siegborn et al. 1991) and likely participates in several efferent systems affecting the control of eye movements, including the vestibuloreticular, commissural, and vestibulocerebellar pathways. The results of anterograde and retrograde labeling studies of vestibulospinal projections are consistent with the idea that some cells in the calretinin area may contribute axons that descend to the spinal cord to influence either sensory or motor function (Nyberg-Hansen 1964; Peterson and Coulter 1977; Blessing et al. 1981, 1987; Holstege and Kuypers 1982; Isu et al. 1996). At least some vestibulospinal projections are inhibitory and GABAergic (Blessing et al. 1987), but both inhibitory and facilitatory influences have been seen, consistent with a cholinergic projection (Isu et al. 1996).

Connections with the reticular formation are suggested by the calretinin-labeled fibers observed streaming between the calretinin area and the reticular formation just ventral to it. Hauglie-Hanssen (1968) also described such fibers in Golgi material in the cat. This region of the reticular formation participates in eye movement control, and is the location of the inhibitory burst neurons (Hikosaka and Kawakami 1977). There are axons from the region that project to the VNC (Pompeiano et al. 1978; Matsuyama et al. 1988). The calretinin-immunoreactive cells may work with the reticular formation in the control of horizontal eye movements.

We saw calretinin-immunoreactive fibers crossing the midline. This observation is in agreement with studies using retrograde tracers that have shown contralaterally projecting

neurons in territory that overlaps the calretinin-immunoreactive area (Pompeiano et al. 1978; Epema et al. 1988). The labeled fibers in the MLF may originate from the cells in the VMN, as suggested by Résibois and Rogers (1992), and interconnect this region with other eye movement way stations.

There is anatomical evidence that suggests that the region of the calretinin area is reciprocally connected with the cerebellum, and specifically the nodulus (Sato et al. 1983; Langer et al. 1985b; Shojaku et al. 1987; Walberg and Dietrichs 1988; Epema et al. 1990; Barmack et al. 1992c; Tan and Gerrits 1992; Tan et al. 1995; Xiong and Matsushita 2000). The notion that the calretinin-immunoreactive cells themselves project to the cerebellum is consistent with the finding of a cholinergic projection from the VNC to the cerebellum (Barmack et al. 1992a, 1992c). However, there are cells immunoreactive for just ChAT interspersed with the cells immunoreactive for both ChAT and calretinin. Direct evidence for the participation of the calretinin-immunoreactive cells in this projection would depend on experiments combining retrograde tracer injections with immunohistochemistry.

Several studies have used retrograde tracing or electrophysiological techniques to locate the cells in the VMN of the cat that project the nuclei of the third, fourth, and sixth cranial nerves (Graybiel and Hartwieg 1974; Gacek 1977; Uchino et al. 1982; Isu and Yokota 1983; Langer et al. 1986; Ohgaki et al. 1988; Spencer et al. 1989; Hoddevik et al. 1991). In all reports, these cells are shown ventral to the calretinin area. This suggests a modulatory rather than a command role for the calretinin area in the generation of eye movements. This idea is also supported by the evidence of connections with the cerebellum, a key source of modulatory information (for example Lisberger 1994).

At present we do not have data to suggest whether single cells in the calretinin area project only to one destination or to several. Nor is the internal organization of the area clear; cells at different A-P levels may have different connections. These questions can only be answered by experiments using retrograde and anterograde tracing techniques.

Medial calbindin region—Consideration of data from several studies suggests that the dense calbindin-immunoreactive patches at the border of the VMN and PH may correspond to areas of dense input from cerebellum, and specifically from the flocculus. Kevetter and Leonard (1997) showed that the two populations of calbindin-labeled fibers were differentially distributed, with cerebellar and not vestibular afferents going to the parvocellular and central subdivisions of the VMN, regions which on geographic grounds would include the dense zones of calbindin fiber immunoreactivity seen in cat. Further evidence for the cerebellum as the source of the calbindin dense fiber patches comes from a study of a mouse mutant that lacks Purkinje cells (Bäurle et al. 1998). That study found that the region at the border of PH and VMN, the site of our dense patch of calbindin-labeled fibers, was free of calbindin-labeled fibers in those animals. Several studies suggest the most likely source of cerebellar projections to the regions of dense calbindin fiber label is the flocculus (Sato et al. 1982; Langer et al. 1985a; Shojaku et al. 1987; Umetani 1992; De Zeeuw et al. 1994; Tan et al. 1995). The calbindin-dense patches thus define input compartments. Anatomical data can suggest possible projections of the cells receiving this input. One likely target is oculomotoneurons, since cells retrogradely labeled from tracer injections in the oculomotor and abducens nuclei have been found in the region of high calbindin density at the border of PH and VMN (Graybiel and Hartwieg 1974; Gacek 1977; Langer et al. 1986). The cerebellar input suggests the possibility that cells receiving that input are brainstem participants in cerebellar-mediated computational or plastic functions (Rambold et al. 2002).

In summary, immunoreactivity for calcium-binding proteins in the cat VNC has shown evidence for two neurochemically-defined subdivisions in the VMN. The calretinin area is

common across several species, whereas the organization of calbindin input fibers shows some species variation. Evidence from anatomy and physiology suggests that these two subdivisions have distinct functional roles in the processing and modulation of vestibular information, and in the control of eye movements. Anatomical studies of the connections of these regions, as well as electrophysiological studies of the constituent neurons, are needed to further develop hypotheses about their function. Especially interesting would be knowledge of the nature of the vestibular signals distributed to these regions. It is clear that axons carrying information from different vestibular end organs have different distributions in the VNC (Stein and Carpenter 1967; Kevetter and Perachio 1985; Siegborn et al. 1991; Sato and Sasaki 1993), but the total pattern is not known. Angaut and Brodal (1967) described the vestibular nuclear complex as a "mosaic of minor units"; immunohistochemistry is adding another anatomical tool for visualizing those units.

Acknowledgements

References

Adams JC. Heavy metal enhancement of DAB-based HRP reaction product. J Histochem Cytochem 1981;29:775. [PubMed: 7252134]

Akaike T. Neuronal organization of the vestibulospinal system in the cat. Brain Res 1983;259:217–227. [PubMed: 6297669]

Angaut P, Brodal A. The projection of the "vestibulocerebellum" onto the vestibular nuclei in the cat. Arch Ital Biol 1967;105:441–479. [PubMed: 5585723]

Arai R, Winsky L, Arai M, Jacobowitz DM. Immunohistochemical localization of calretinin in the rat hindbrain. J Comp Neurol 1991;310:21–44. [PubMed: 1939729]

Baimbridge KG, Celio MR, Rogers JH. Calcium-binding proteins in the nervous system. Trends Neurosci 1992;15:303–308. [PubMed: 1384200]

Baizer J, Baker J. Calretinin immunoreactivity in the vestibular nuclear complex of the cat. Neurosci Abstr 2000;26:1493.

Baizer JS, Baker JF. Distribution of cholinergic cells in the vestibular nuclear complex of the cat. Neurosci Abstr 2001;27:785.

Baker J, Goldberg J, Hermann G, Peterson B. Spatial and temporal response properties of secondary neurons that receive convergent input in vestibular nuclei of alert cats. Brain Res 1984;294:138–143. [PubMed: 6697230]

Baker R, Berthoz A. Is the prepositus hypoglossi nucleus the source of another vestibulo-ocular pathway? Brain Res 1975;86:121–127. [PubMed: 163664]

Bankoul S, Neuhuber WL. A direct projection from the medial vestibular nucleus to the cervical spinal dorsal horn of the rat, as demonstrated by anterograde and retrograde tracing. Anat Embryol (Berl) 1992;185:77–85. [PubMed: 1736687]

Barmack NH. Central vestibular system: vestibular nuclei and posterior cerebellum. Brain Res Bull 2003;60:511–541. [PubMed: 12787870]

Barmack NH, Baughman RW, Eckenstein FP. Cholinergic innervation of the cerebellum of rat, rabbit, cat, and monkey as revealed by choline acetyltransferase activity and immunohistochemistry. J Comp Neurol 1992a;317:233–249. [PubMed: 1577998]

Barmack NH, Baughman RW, Eckenstein FP. Cholinergic innervation of the cerebellum of the rat by secondary vestibular afferents. Ann NY Acad Sci 1992b;656:566–579. [PubMed: 1376098]

Barmack NH, Baughman RW, Eckenstein FP, Shojaku H. Secondary vestibular cholinergic projection to the cerebellum of rabbit and rat as revealed by choline acetyltransferase immunohistochemistry, retrograde and orthograde tracers. J Comp Neurol 1992c;317:250–270. [PubMed: 1577999]

Batini C. Cerebellar localization and colocalization of GABA and calcium binding protein-D28K. Arch Ital Biol 1990;128:127–149. [PubMed: 2268180]

Bäurle J, Vogten H, Grüsser-Cornehls U. Course and targets of the calbindin D-28k subpopulation of primary vestibular afferents. J Comp Neurol 1998;402:111–128. [PubMed: 9831049]

Berman A (1968) The brain stem of the cat. University of Wisconsin Press, Madison, WI

Blessing WW, Goodchild AK, Dampney RA, Chalmers JP. Cell groups in the lower brain stem of the rabbit projecting to the spinal cord, with special reference to catecholamine-containing neurons. Brain Res 1981;221:35–55. [PubMed: 6168336]

Blessing WW, Hedger SC, Oertel WH. Vestibulospinal pathway in rabbit includes GABA-synthesizing neurons. Neurosci Lett 1987;80:158–162. [PubMed: 3317134]

Boyle R. Morphology of lumbar-projecting lateral vestibulospinal neurons in the brainstem and cervical spinal cord in the squirrel monkey. Arch Ital Biol 2000;138:107–122. [PubMed: 10782253]

Boyle R, Belton T, McCrea RA. Responses of identified vestibulospinal neurons to voluntary eye and head movements in the squirrel monkey. Ann NY Acad Sci 1996;781:244–263. [PubMed: 8694418]

Brodal A. The vestibular nuclei in the macaque monkey. J Comp Neurol 1984;227:252–266. [PubMed: 6470216]

Brodal A, Pompeiano O. The vestibular nuclei in the cat. J Anatomy 1957;91:438–454.

Carleton SC, Carpenter MB. Distribution of primary vestibular fibers in the brainstem and cerebellum of the monkey. Brain Res 1984;294:281–298. [PubMed: 6200186]

Carpenter MB, Huang Y, Pereira AB, Hersh LB. Immunocytochemical features of the vestibular nuclei in the monkey and cat. J Hirnforsch 1990;31:585–599. [PubMed: 1707074]

Celio MR. Calbindin D-28k and parvalbumin in the rat nervous system. Neuroscience 1990;35:375–475. [PubMed: 2199841]

Chevalier G, Mana S. Honeycomb-like structure of the intermediate layers of the rat superior colliculus, with additional observations in several other mammals: AChE patterning. J Comp Neurol 2000;419:137–153. [PubMed: 10722995]

Condé F, Lund JS, Jacobowitz DM, Baimbridge KG, Lewis DA. Local circuit neurons immunoreactive for calretinin, calbindin D-28k or parvalbumin in monkey prefrontal cortex: distribution and morphology. J Comp Neurol 1994;341:95–116. [PubMed: 8006226]

Cusick CG, Scripter JL, Darensbourg JG, Weber JT. Chemoarchitectonic subdivisions of the visual pulvinar in monkeys and their connectional relations with the middle temporal and rostral dorsolateral visual areas, MT and DLr. J Comp Neurol 1993;336:1–30. [PubMed: 8254107]

de Venecia RK, Smelser CB, Lossman SD, McMullen NT. Complementary expression of parvalbumin and calbindin D-28k delineates subdivisions of the rabbit medial geniculate body. J Comp Neurol 1995;359:595–612. [PubMed: 7499550]

De Zeeuw CI, Wylie DR, DiGiorgi PL, Simpson JI. Projections of individual Purkinje cells of identified zones in the flocculus to the vestibular and cerebellar nuclei in the rabbit. J Comp Neurol 1994;349:428–447. [PubMed: 7852634]

Dickman JD, Angelaki DE. Vestibular convergence patterns in vestibular nuclei neurons of alert primates. J Neurophysiol 2002;88:3518–3533. [PubMed: 12466465]

Donevan AH, MacDonald JA, Brennan PA, Rose PK. Morphology of single vestibulospinal collaterals in the upper cervical spinal cord of the cat. II. Collaterals originating from axons outside the ventral funiculi. J Comp Neurol 1992;322:343–359. [PubMed: 1517484]

Edmonds B, Reyes R, Schwaller B, Roberts WM. Calretinin modifies presynaptic calcium signaling in frog saccular hair cells. Nat Neurosci 2000;3:786–790. [PubMed: 10903571]

Epema AH, Gerrits NM, Voogd J. Commissural and intrinsic connections of the vestibular nuclei in the rabbit: a retrograde labeling study. Exp Brain Res 1988;71:129–146. [PubMed: 2458274]

Epema AH, Gerrits NM, Voogd J. Secondary vestibulocerebellar projections to the flocculus and uvulo-nodular lobule of the rabbit: a study using HRP and double fluorescent tracer techniques. Exp Brain Res 1990;80:72–82. [PubMed: 2358039]

Fortin M, Marchand R, Parent A. Calcium-binding proteins in primate cerebellum. Neurosci Res 1998;30:155–168. [PubMed: 9579649]

Gacek RR. Location of brain stem neurons projecting to the oculomotor nucleus in the cat. Exp Neurol 1977;57:725–749. [PubMed: 923675]

Gacek RR, Lyon M. The localization of vestibular efferent neurons in the kitten with horseradish peroxidase. Acta Otolaryngol 1974;77:92–101. [PubMed: 4133485]

Gerrits N (1990) Vestibular nuclear complex. In: The human nervous system. Academic, Philadelphia, PA, pp 863–888

Graybiel AM. Compartmental organization of the mammalian striatum. Prog Brain Res 1983;58:247–256. [PubMed: 6635191]

Graybiel AM, Hartwieg EA. Some afferent connections of the oculomotor complex in the cat: an experimental study with tracer techniques. Brain Res 1974;81:543–551. [PubMed: 4434207]

Graybiel AM, Ragsdale CW Jr. Histochemically distinct compartments in the striatum of human, monkeys, and cat demonstrated by acetylthiocholinesterase staining. P Natl Acad Sci USA 1978;75:5723–5726.

Hauglie-Hanssen E. Intrinsic neuronal organization of the vestibular nuclear complex in the cat. A Golgi study. Ergeb Anat Entwicklungsgesch 1968;40:3–105. [PubMed: 4178473]

Highstein SM, Ito M. Differential localization within the vestibular nuclear complex of the inhibitory and excitatory cells innervating 3d nucleus oculomotor neurons in rabbit. Brain Res 1971;29:358–362. [PubMed: 4329991]

Hikosaka O, Kawakami T. Inhibitory reticular neurons related to the quick phase of vestibular nystagmus -their location and projection. Exp Brain Res 1977;27:377–386. [PubMed: 880992]

Hockfield S (1993) Selected methods for antibody and nucleic acid probes. Cold Spring Harbor Laboratory Press, Plainview, NY

Hoddevik GH, Dietrichs E, Walberg F. Afferent connections to the abducent nucleus in the cat. Arch Ital Biol 1991;129:63–72. [PubMed: 1707258]

Holstege G, Kuypers HG. The anatomy of brain stem pathways to the spinal cord in cat. A labeled amino acid tracing study. Prog Brain Res 1982;57:145–175. [PubMed: 7156396]

Horn AK, Büttner-Ennever JA. Premotor neurons for vertical eye movements in the rostral mesencephalon of monkey and human: histologic identification by parvalbumin immunostaining. J Comp Neurol 1998;392:413–427. [PubMed: 9514507]

Horn AK, Büttner-Ennever JA, Suzuki Y, Henn V. Histological identification of premotor neurons for horizontal saccades in monkey and man by parvalbumin immunostaining. J Comp Neurol 1995;359:350–363. [PubMed: 7499534]

Horn AK, Büttner U, Büttner-Ennever JA. Brainstem and cerebellar structures for eye movement generation. Adv Otorhino-laryng 1999;55:1–25.

Horton JC, Hubel DH. Regular patchy distribution of cytochrome oxidase staining in primary visual cortex of macaque monkey. Nature 1981;292:762–764. [PubMed: 6267472]

Imagawa M, Isu N, Sasaki M, Endo K, Ikegami H, Uchino Y. Axonal projections of utricular afferents to the vestibular nuclei and the abducens nucleus in cats. Neurosci Lett 1995;186:87–90. [PubMed: 7777205]

Isu N, Yokota J. Morphophysiological study on the divergent projection of axon collaterals of medial vestibular nucleus neurons in the cat. Exp Brain Res 1983;53:151–162. [PubMed: 6673993]

Isu N, Thomson DB, Wilson VJ. Vestibulospinal effects on neurons in different regions of the gray matter of the cat upper cervical cord. J Neurophysiol 1996;76:2439–2446. [PubMed: 8899616]

Jeon MH, Jeon CJ. Immunocytochemical localization of calretinin containing neurons in retina from rabbit, cat, and dog. Neurosci Res 1998;32:75–84. [PubMed: 9831254]

Jones EG, Dell'Anna ME, Molinari M, Rausell E, Hashikawa T. Subdivisions of macaque monkey auditory cortex revealed by calcium-binding protein immunoreactivity. J Comp Neurol 1995;362:153–170. [PubMed: 8576431]

Kaneko CR. Eye movement deficits after ibotenic acid lesions of the nucleus prepositus hypoglossi in monkeys. I. Saccades and fixation. J Neurophysiol 1997;78:1753–1768. [PubMed: 9325345]

Kaneko CR. Eye movement deficits following ibotenic acid lesions of the nucleus prepositus hypoglossi in monkeys II. Pursuit, vestibular, and optokinetic responses. J Neurophysiol 1999;81:668–681. [PubMed: 10036269]

Kevetter GA. Pattern of selected calcium-binding proteins in the vestibular nuclear complex of two rodent species. J Comp Neurol 1996;365:575–584. [PubMed: 8742303]

Kevetter GA, Leonard RB. Use of calcium-binding proteins to map inputs in vestibular nuclei of the gerbil. J Comp Neurol 1997;386:317–327. [PubMed: 9295155]

Kevetter GA, Perachio AA. Central projections of first order vestibular neurons innervating the sacculus and posterior canal in the gerbil. Prog Clin Biol Res 1985;176:279–291. [PubMed: 4001140]

Kimura H, McGeer PL, Peng JH, McGeer EG. The central cholinergic system studied by choline acetyltransferase immunohistochemistry in the cat. J Comp Neurol 1981;200:151–201. [PubMed: 7287919]

Kokkoroyannis T, Scudder CA, Balaban CD, Highstein SM, Moschovakis AK. Anatomy and physiology of the primate interstitial nucleus of Cajal I. efferent projections. J Neurophysiol 1996;75:725–739. [PubMed: 8714648]

Korte GE. The brainstem projection of the vestibular nerve in the cat. J Comp Neurol 1979;184:279–292. [PubMed: 762285]

Krutki P, Jankowska E, Edgley SA. Are crossed actions of reticulospinal and vestibulospinal neurons on feline motoneurons mediated by the same or separate commissural neurons? J Neurosci 2003;23:8041–8050. [PubMed: 12954866]

Kuze B, Matsuyama K, Matsui T, Miyata H, Mori S. Segment-specific branching patterns of single vestibulospinal tract axons arising from the lateral vestibular nucleus in the cat: A PHA-L tracing study. J Comp Neurol 1999;414:80–96. [PubMed: 10494080]

Langer T, Fuchs AF, Chubb MC, Scudder CA, Lisberger SG. Floccular efferents in the rhesus macaque as revealed by autoradiography and horseradish peroxidase. J Comp Neurol 1985a;235:26–37. [PubMed: 3989003]

Langer T, Fuchs AF, Scudder CA, Chubb MC. Afferents to the flocculus of the cerebellum in the rhesus macaque as revealed by retrograde transport of horseradish peroxidase. J Comp Neurol 1985b;235:1–25. [PubMed: 3989000]

Langer T, Kaneko CR, Scudder CA, Fuchs AF. Afferents to the abducens nucleus in the monkey and cat. J Comp Neurol 1986;245:379–400. [PubMed: 3082944]

Leblond H, Menard A, Gossard JP. Bulbospinal control of spinal cord pathways generating locomotor extensor activities in the cat. J Physiol 2000;525(1):225–240. [PubMed: 10811739]

Lenzi D, Roberts WM. Calcium signalling in hair cells: multiple roles in a compact cell. Curr Opin Neurobiol 1994;4:496–502. [PubMed: 7812137]

Lisberger SG. Neural basis for motor learning in the vestibuloocular reflex of primates. III. Computational and behavioral analysis of the sites of learning. J Neurophysiol 1994;72:974–998. [PubMed: 7983549]

Matsuyama K, Ohta Y, Mori S. Ascending and descending projections of the nucleus reticularis gigantocellularis in the cat demonstrated by the anterograde neural tracer, Phaseolus vulgaris leucoagglutinin (PHA-L). Brain Res 1988;460:124–141. [PubMed: 2464400]

McCrea RA, Strassman A, Highstein SM. Anatomical and physiological characteristics of vestibular neurons mediating the vertical vestibulo-ocular reflexes of the squirrel monkey. J Comp Neurol 1987a;264:571–594. [PubMed: 2824575]

McCrea RA, Strassman A, May E, Highstein SM. Anatomical and physiological characteristics of vestibular neurons mediating the horizontal vestibulo-ocular reflex of the squirrel monkey. J Comp Neurol 1987b;264:547–570. [PubMed: 2824574]

McCrea RA, Gdowski GT, Boyle R, Belton T. Firing behavior of vestibular neurons during active and passive head movements: vestibulo-spinal and other non-eye-movement related neurons. J Neurophysiol 1999;82:416–428. [PubMed: 10400968]

Mitsacos A, Reisine H, Highstein SM. The superior vestibular nucleus: an intracellular HRP study in the cat. I. Vestibuloocular neurons. J Comp Neurol 1983;215:78–91. [PubMed: 6853767]

Moreno-Lopez B, Escudero M, De Vente J, Estrada C. Morphological identification of nitric oxide sources and targets in the cat oculomotor system. J Comp Neurol 2001;435:311–324. [PubMed: 11406814]

Murakawa R, Kosaka T. Diversity of the calretinin immunoreactivity in the dentate gyrus of gerbils, hamsters, guinea pigs, and laboratory shrews. J Comp Neurol 1999;411:413–430. [PubMed: 10413776]

Naito Y, Newman A, Lee WS, Beykirch K, Honrubia V. Projections of the individual vestibular end-organs in the brain stem of the squirrel monkey. Hearing Res 1995;87:141–155.

Newlands SD, Perachio AA. Central projections of the vestibular nerve: a review and single fiber study in the Mongolian gerbil. Brain Res Bull 2003;60:475–495. [PubMed: 12787868]

Nyberg-Hansen R. Origin and termination of fibers from the vestibular nuclei descending in the medial longitudinal fasciculus. An experimental study with silver impregnation methods in the cat. J Comp Neurol 1964;122:355–367. [PubMed: 14184859]

Ohgaki T, Curthoys IS, Markham CH. Morphology of physiologically identified second-order vestibular neurons in cat, with intracellularly injected HRP. J Comp Neurol 1988;276:387–411. [PubMed: 3192768]

Paxinos G, Carrive P, Wang H, Wang P-Y (1999) Chemoarchitectonic atlas of the rat brainstem. Academic, San Diego, CA

Peterson BW, Coulter JD. A new long spinal projection from the vestibular nuclei in the cat. Brain Res 1977;122:351–356. [PubMed: 837234]

Pompeiano O, Mergner T, Corvaja N. Commissural, perihypoglossal and reticular afferent projections to the vestibular nuclei in the cat. An experimental anatomical study with the method of the retrograde transport of horseradish peroxidase. Arch Ital Biol 1978;116:130–172. [PubMed: 80203]

Rambold H, Churchland A, Selig Y, Jasmin L, Lisberger SG. Partial ablations of the flocculus and ventral paraflocculus in monkeys cause linked deficits in smooth pursuit eye movements and adaptive modification of the VOR. J Neurophysiol 2002;87:912–924. [PubMed: 11826056]

Rausell E, Jones EG. Chemically distinct compartments of the thalamic VPM nucleus in monkeys relay principal and spinal trigeminal pathways to different layers of the somato-sensory cortex. J Neurosci 1991a;11:226–237. [PubMed: 1702464]

Rausell E, Jones EG. Histochemical and immunocytochemical compartments of the thalamic VPM nucleus in monkeys and their relationship to the representational map. J Neurosci 1991b;11:210–225. [PubMed: 1846010]

Rausell E, Bae CS, Vinuela A, Huntley GW, Jones EG. Calbindin and parvalbumin cells in monkey VPL thalamic nucleus: distribution, laminar cortical projections, and relations to spinothalamic terminations. J Neurosci 1992;12:4088–4111. [PubMed: 1328563]

Résibois A, Rogers JH. Calretinin in rat brain: an immunohistochemical study. Neuroscience 1992;46:101–134. [PubMed: 1594096]

Roberts WM. Spatial calcium buffering in saccular hair cells. Nature 1993;363:74–76. [PubMed: 8479539]

Roberts WM. Localization of calcium signals by a mobile calcium buffer in frog saccular hair cells. J Neurosci 1994;14:3246–3262. [PubMed: 8182469]

Rogers JH, Résibois A. Calretinin and calbindin-D-28k in rat brain: patterns of partial co-localization. Neuroscience 1992;51:843–865. [PubMed: 1488126]

Rose PK, Tourond JA, Donevan AH. Morphology of single vestibulospinal collaterals in the upper cervical spinal cord of the cat: III collaterals originating from axons in the ventral funiculus ipsilateral to their cells of origin. J Comp Neurol 1996;364:16–31. [PubMed: 8789273]

Sato F, Sasaki H. Morphological correlations between spontaneously discharging primary vestibular afferents and vestibular nucleus neurons in the cat. J Comp Neurol 1993;333:554–566. [PubMed: 8370817]

Sato Y, Kawasaki T, Ikarashi K. Zonal organization of the floccular Purkinje cells projecting to the vestibular nucleus in cats. Brain Res 1982;232:1–15. [PubMed: 6173097]

Sato Y, Kawasaki T, Ikarashi K. Afferent projections from the brainstem to the three floccular zones in cats. II. Mossy fiber projections. Brain Res 1983;272:37–48. [PubMed: 6616198]

Saxon DW, Beitz AJ. The normal distribution and projections of constitutive NADPH-d/NOS neurons in the brainstem vestibular complex of the rat. J Comp Neurol 2000;425:97–120. [PubMed: 10940945]

Shamboul KM. Lumbosacral predominance of vestibulospinal fibre projection in the rat. J Comp Neurol 1980;192:519–530. [PubMed: 7419742]

Shojaku H, Sato Y, Ikarashi K, Kawasaki T. Topographical distribution of Purkinje cells in the uvula and the nodulus projecting to the vestibular nuclei in cats. Brain Res 1987;416:100–112. [PubMed: 3620947]

Siegborn J, Yingcharoen K, Grant G. Brainstem projections of different branches of the vestibular nerve: an experimental study by transganglionic transport of horseradish peroxidase in the cat. II. The anterior and posterior ampullar nerves. Anat Embryol (Berl) 1991;184:291–299. [PubMed: 1793167]

Sillitoe RV, Hulliger M, Dyck R, Hawkes R. Antigenic compartmentation of the cat cerebellar cortex. Brain Res 2003;977:1–15. [PubMed: 12788507]

Spencer RF, Wenthold RJ, Baker R. Evidence for glycine as an inhibitory neurotransmitter of vestibular, reticular, and prepositus hypoglossi neurons that project to the cat abducens nucleus. J Neurosci 1989;9:2718–2736. [PubMed: 2570136]

Stein BM, Carpenter MB. Central projections of portions of the vestibular ganglia innervating specific parts of the labyrinth of the rhesus monkey. Am J Anat 1967;120:281–318.

Taber E. The cytoarchitecture of the brain stem of the cat. I. Brain stem nuclei of cat. J Comp Neurol 1961;116:27–69. [PubMed: 13774738]

Tan H, Gerrits NM. Laterality in the vestibulo-cerebellar mossy fiber projection to flocculus and caudal vermis in the rabbit: a retrograde fluorescent double-labeling study. Neuroscience 1992;47:909–919. [PubMed: 1374542]

Tan J, Gerrits NM, Nanhoe R, Simpson JI, Voogd J. Zonal organization of the climbing fiber projection to the flocculus and nodulus of the rabbit: a combined axonal tracing and acetylcholinesterase histochemical study. J Comp Neurol 1995;356:23–50. [PubMed: 7543121]

Uchino Y, Hirai N, Suzuki S. Branching pattern and properties of vertical- and horizontal-related excitatory vestibuloocular neurons in the cat. J Neurophysiol 1982;48:891–903. [PubMed: 6292373]

Umetani T. Efferent projections from the flocculus in the albino rat as revealed by an autoradiographic orthograde tracing method. Brain Res 1992;586:91–103. [PubMed: 1324779]

Van Brederode JF, Mulligan KA, Hendrickson AE. Calcium-binding proteins as markers for subpopulations of GABAergic neurons in monkey striate cortex. J Comp Neurol 1990;298:1–22. [PubMed: 2170466]

Walberg F, Dietrichs E. The interconnection between the vestibular nuclei and the nodulus: a study of reciprocity. Brain Res 1988;449:47–53. [PubMed: 2456133]

Wilson VJ, Melvill Jones G (1979) Mammalian vestibular physiology. Plenum, New York

Wilson VJ, Schor RH. The neural substrate of the vestibulocollic reflex. What needs to be learned. Exp Brain Res 1999;129:483–493. [PubMed: 10638422]

Wilson VJ, Zarzecki P, Schor RH, Isu N, Rose PK, Sato H, Thomson DB, Umezaki T. Cortical influences on the vestibular nuclei of the cat. Exp Brain Res 1999;125:1–13. [PubMed: 10100970]

Xiong G, Matsushita M. Connections of Purkinje cell axons of lobule X with vestibulocerebellar neurons projecting to lobule X or IX in the rat. Exp Brain Res 2000;133:219–228. [PubMed: 10968222]

Zhang X, Zakir M, Meng H, Sato H, Uchino Y. Convergence of the horizontal semicircular canal and otolith afferents on cat single vestibular neurons. Exp Brain Res 2001;140:1–11. [PubMed: 11500792]

Zhang Y, Partsalis AM, Highstein SM. Properties of superior vestibular nucleus neurons projecting to the cerebellar flocculus in the squirrel monkey. J Neurophysiol 1993;69:642–645. [PubMed: 8459292]

Zhang Y, Partsalis AM, Highstein SM. Properties of superior vestibular nucleus flocculus target neurons in the squirrel monkey. I. General properties in comparison with flocculus projecting neurons. J Neurophysiol 1995;73:2261–2278. [PubMed: 7666137]
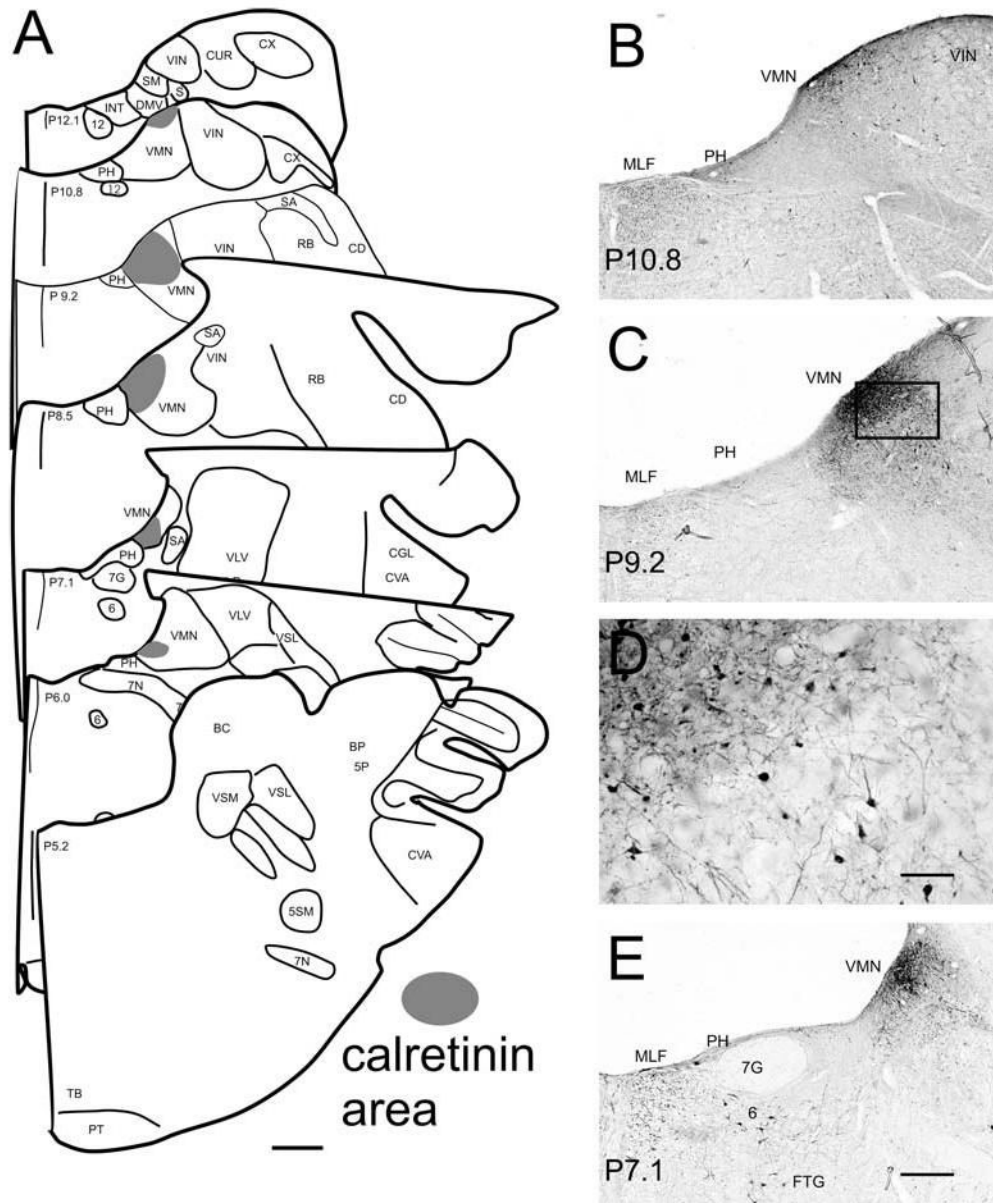
Fig. 1.
A The dense calretinin-immunoreactive area (*shaded*) shown on drawings of seven frontal sections through the vestibular nuclear complex from about P12 to P5 based on Berman (1968). **B, C, E** The calretinin area shown in photomicrographs on three frontal sections at different A-P levels. Also visible are scattered labeled cells outside this region in the VMN (B, C, D), labeled cells in VIN (B, C), labeled fibers in the MLF (B, C, E), and labeled cells in PH (B, C), and the abducens nucleus and reticular formation (E). The numbers at the bottom left of each panel show the approximate stereotaxic level of the section. **D** Higher magnification photomicrograph of the boxed region in C, showing the difference between the more dense central region, *upper left*, and more lightly labeled surrounding region, *lower right*. Both regions are included in the shaded areas in the schematics in A. Scale bars: A 1 mm, D 200 μm, B, C, E 500 μm
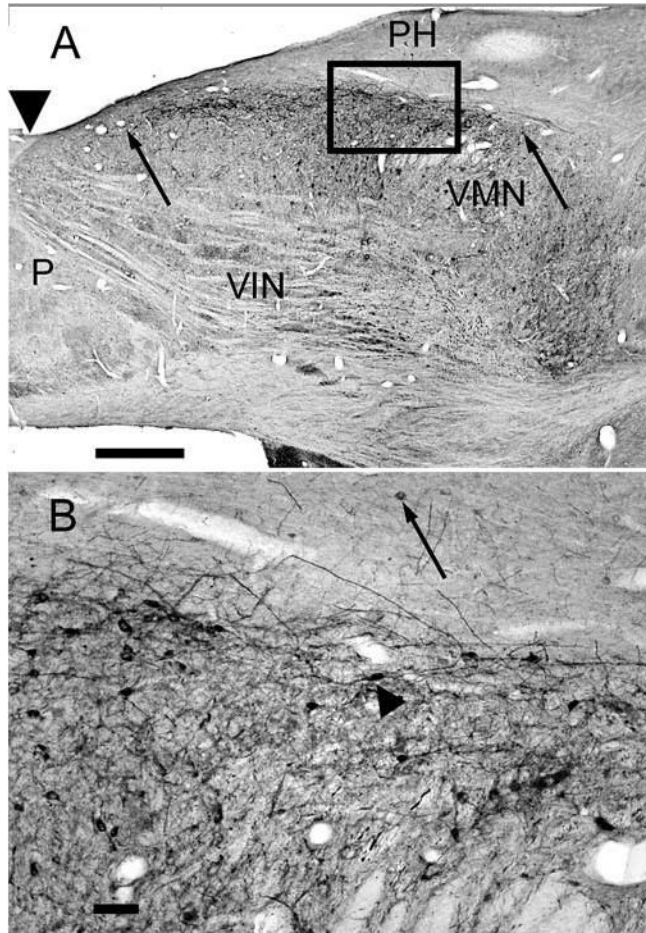
Fig. 2.
A The calretinin area in the VMN on a horizontal section at about −3.4. The anterior and posterior limits of the calretinin area are indicated by *arrows*. Note scattered labeled cells in the bordering nuclei VIN and PH. *Arrowhead* indicates an A-P level of about P14. **B** Higher magnification photomicrograph of the boxed area in A showing cells and processes in the calretinin area; the *arrowhead* points to a cell with a fusiform cell body. The *arrow* indicates a labeled cell in PH. Note the anterior-posterior orientation of the longer dendrites. *P* is posterior. *Scale bars* A 1 mm, B 100 μm
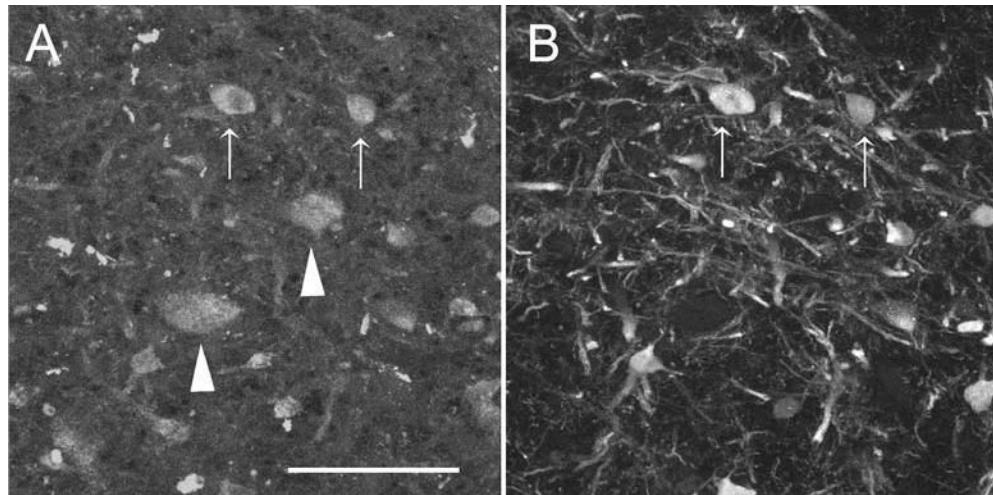
Fig. 3.
Colocalization of calretinin and ChAT in cells in the calretinin-immunoreactive area. **A** ChAT-immunoreactive cell bodies in the calretinin area at about P10. The *arrows* show two cell bodies that are also calretinin-immunoreactive; the *arrowheads* show cells which are not. **B** Calretinin-immunoreactive cells and fibers in the calretinin area. The *arrows* indicate the same cells shown in A. Scale bar: 50 μm
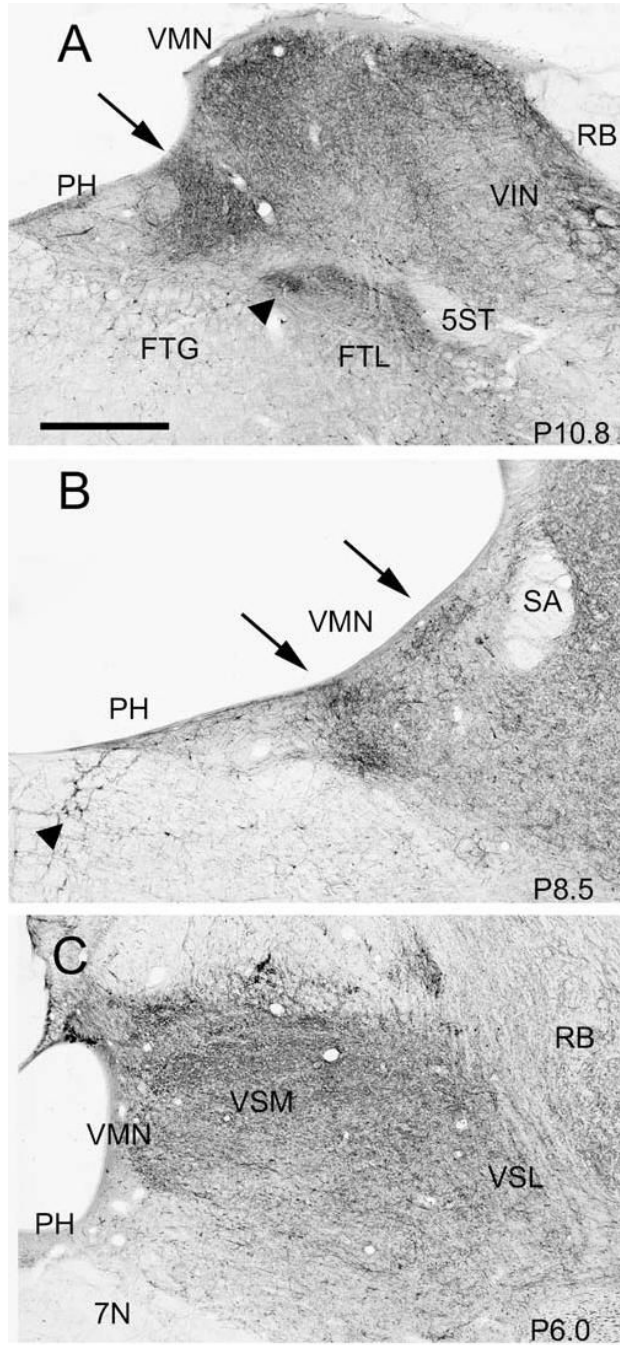
Fig. 4.
Changes in the pattern of calbindin-immunoreactivity in the VNC at different A-P levels,
shown on three photomicrographs. The stereotaxic location of each section is indicated in the
bottom right of each panel. **A** *Arrow* shows the trapezoidal calbindin-immunoreactive dense
patch; *arrowhead* shows a small region of dense label in the reticular formation. Also visible
are denser labeling along the ventricle in VMN and VIN. **B** The *arrow* on the *left* shows the
two dense patches of label at the border of VMN and PH, and the *arrow* on the *right* the dense
label along the ventricle. *Arrowhead* shows large calbindin-immunoreactive cell bodies
embedded in the MLF. **C** Relatively uniform label in VMN and the VSM and VSL. Scale bar:
500 μm
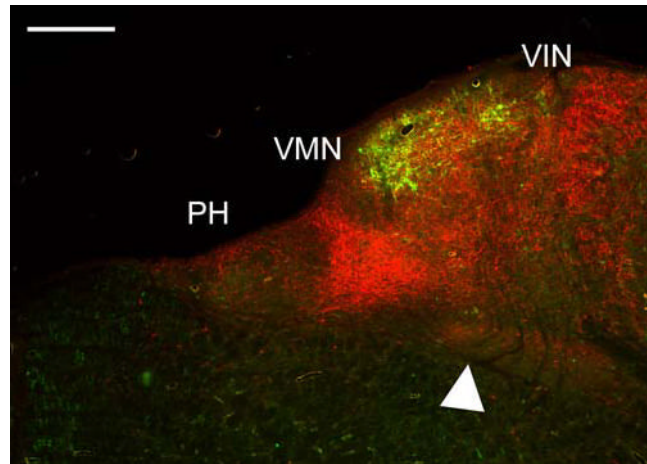
Fig. 5.
Relative distributions of calretinin-immunoreactivity (*green*) and calbindin-immunoreactivity (*red*) on a section at about P11, at about the same level illustrated in Fig. 4A. Calretinin label is primarily in cells; calbindin label primarily in fibers. *Arrowhead* points to the dense calbindin cell label in the reticular formation. Scale bar: 500 μm
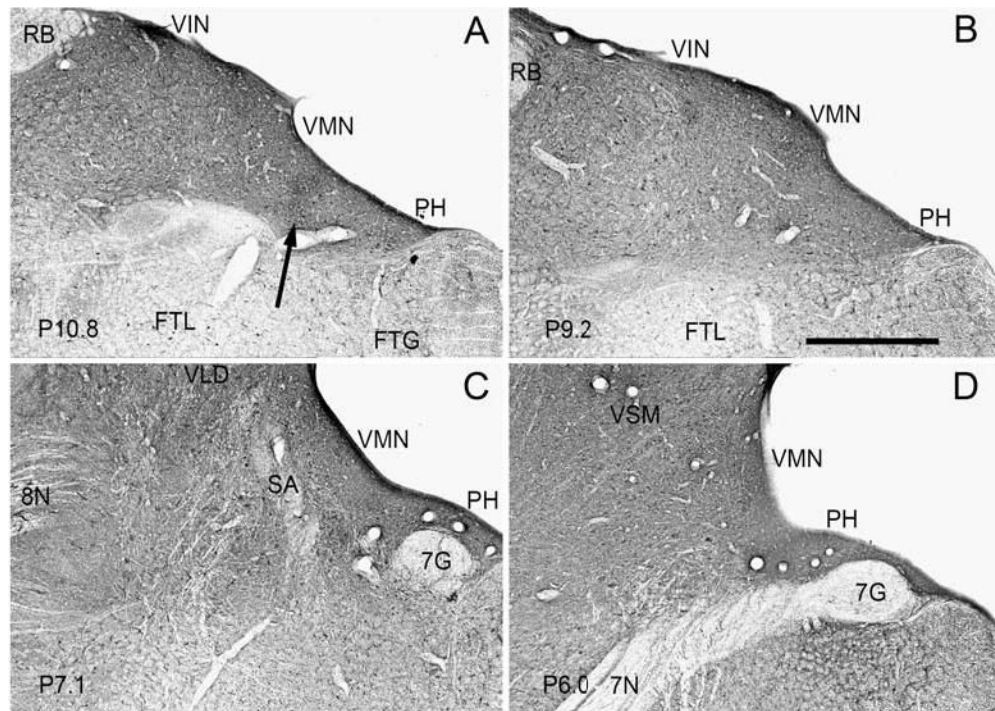
Fig. 6.
Widespread and uniform parvalbumin-immunoreactivity, predominantly in fibers and puncta, in all nuclei of the VNC shown on four photomicrographs at the stereotaxic levels indicated in the lower left corner of each panel. **A** Label in VMN, VIN and PH. *Arrow* shows the darker patch of label at the border of VMN and PH. **B** Uniform label in VMN, VIN and PH. **C** Uniform label in the VMN and VLD. **D** Uniform label in the VMN and VSM. Scale bar: 1 mm
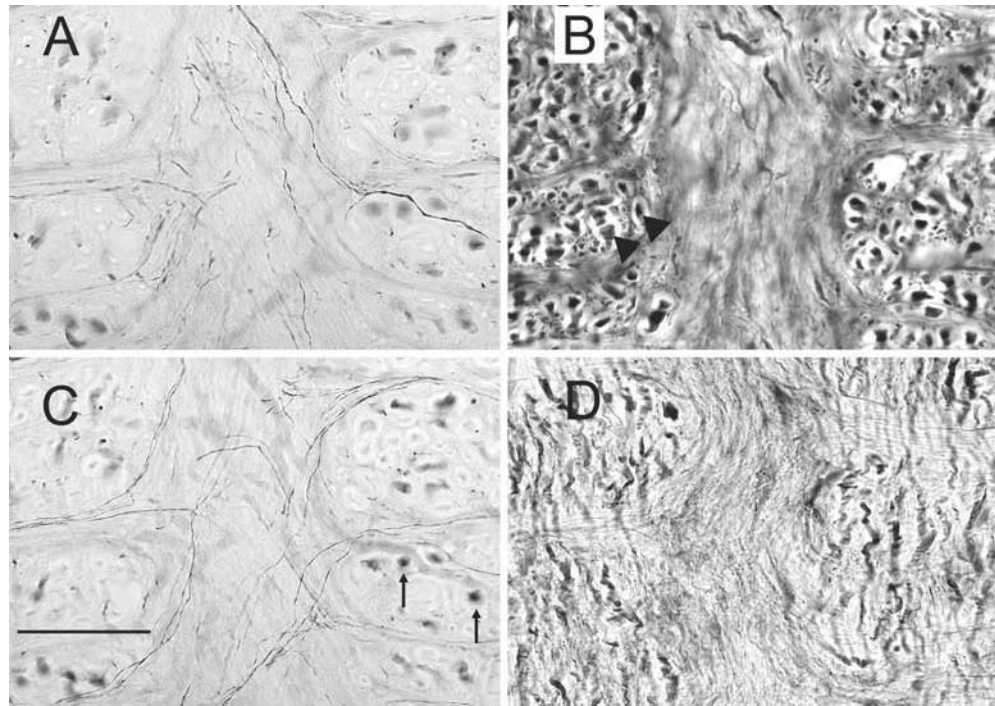
Fig. 7.
Immunoreactivity for each of the calcium-binding proteins in and around the MLF; all sections are at about P9. **A, C** Calretinin-immunoreactivity shown in two photomicrographs of the same location at different planes of focus. There are fine-labeled fibers crossing the midline, and large stained fibers in the MLF cut in cross-section (*arrows*). **B** Parvalbumin-immunoreactive fibers in the MLF showing the densely-stained large diameter fibers (*arrowheads*) cut in cross-section. **D** Calbindin-immunoreactivity in the MLF; a few fine fibers cross the MLF, and there are short stained fibers with a dorsal-ventral orientation. Scale bar: 100 μm
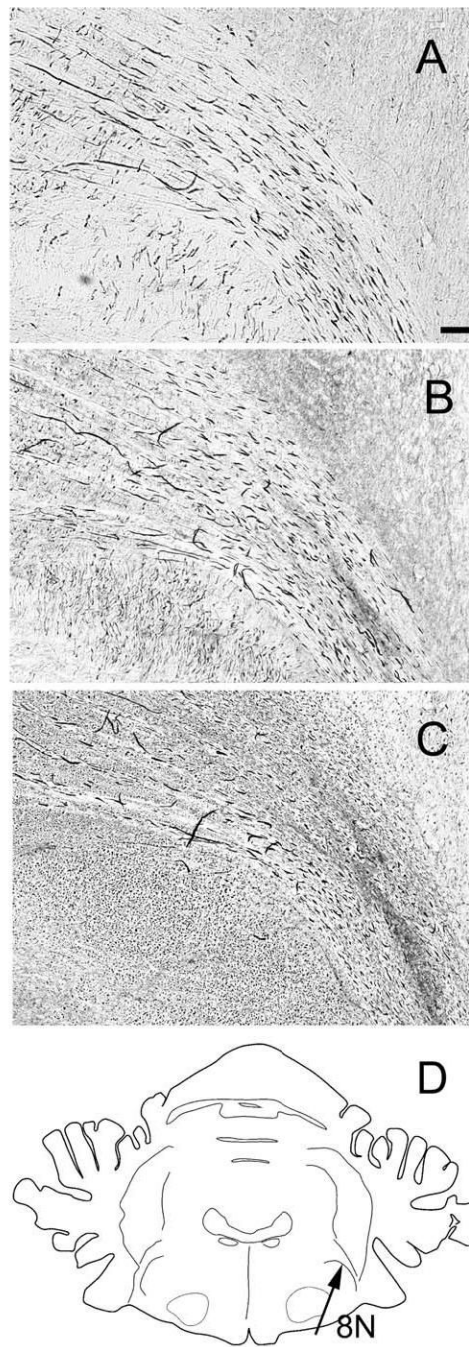
Fig. 8.
Immunoreactivity for calcium-binding proteins in the fibers of the eighth nerve as it enters the brainstem, shown on photomicrographs of neighboring sections at about P7.0. **A** Calretinin-immunoreactive fibers. **B** Calbindin-immunoreactive fibers. **C** Parvalbumin-immunoreactive fibers. **D** The drawing shows an outline of a section through the brainstem at P7.